The smart PFD with LRB for seismic protection of the horizontally curved bridge

N.P. Kataria[*] and R.S. Jangid

Department of Civil Engineering, Indian Institute of Technology Bombay, Powai, Mumbai - 400 076, India

Abstract. Recently, number of smart material are investigated and widely used in civil construction and other industries. Present study investigates the application of smart semi-active piezoelectric friction damper (PFD) made with piezoelectric material for the seismic control of the horizontally curved bridge isolated with lead rubber bearing (LRB). The main aim of the study is to investigate the effectiveness of hybrid system and to find out the optimum parameters of PFD for seismic control of the curved bridge. The selected curved bridge is a continuous three-span concrete box girder supported on pier and rigid abutment. The PFD is located between the deck and abutments or piers in chord and radial directions. The bridge is excited with four different earthquake ground motions with all three components (i.e. two horizontal and a vertical) having different characteristics. It is observed that the use of semi-active PFD with LRB is quite effective in controlling the response of the curved bridge as compared with passive system. The incorporation of the smart damper requiring small amount of energy in addition with an isolation system can be used for effective control the curved bridge against the dynamic loading.

Keywords: seismic isolation; PFD; LRB; curved bridge; seismic analysis

1. Introduction

Recently, numbers of smart material have been investigated by the researcher. These materials include piezoelectric materials, magneto-rheological material, shape memory alloys, electro-rheological materials, etc. and these are widely used in aerospace, medical application, leisure industries, robotics and civil engineering field. Use of smart material in protecting the structure against the catastrophic earthquake will not only help with the safety of human life but also the protection of lifeline structures. The salient feature of a friction damper such as huge dissipation of energy by virtue of friction and simple in operation attracts the researcher for use in the seismic control of structures. Chen and Chen (2000) introduced the combination of friction damper with smart material (piezoelectric) for a seismic control of different structure. In conventional friction dampers, frictional force fluctuates suddenly between stick and slip states, whereas in the Piezoelectric friction damper (PFD), it changes smoothly and continuously. The

---

∗Corresponding author, Ph.D. Student, E-mail: nkataria143@gmail.com
[a] Ph.D. Student
[b] Professor, E-mail: rsjangid@civil.iitb.ac.in

PFD produces the controllable frictional force with adjusting frictional characteristics by utilizing the response of structure. The PFD has unique characteristics such as simplicity, reliability, compactness, high-speed actuation, low power consumption with effectiveness over wide frequency bands (Chen and Chen 2000) which make it unique for seismic control of civil structure. The controlling friction force in the damper is regulated by using piezoelectric stack actuators. This piezoelectric stack made up with piezoelectric material having a unique property as to produce an electric current when they are placed under mechanical stress. The piezoelectric process is also reversible, so if an electric current applied to these materials, they will change shape slightly and generate a significant amount of stress. When piezoelectric actuators subjected to driven command such as a current or voltage signal responds rapidly and accurately produces a large force, while maintaining low displacements.

A number of researchers used the PFD in different structures with different controlling algorithm and evaluated its effectiveness. Chen and Chen (2000, 2002, 2004) found the effectiveness of PFD in seismic control of 20 storey building, and also perform experiments on quarter-scale three-storey building model equipped with PFD. It was found that the semi-active PFD with slight saturation is beneficial to the mitigation of building responses with substantially less external power than its associated active damper. Ozbulut and Hurlebaus (2010) developed and used the fuzzy logic controllers for PFD for seismic protection of base-isolated buildings. It was found that the developed fuzzy logic controllers can be effectively reduced isolation system deformations without the loss of the potential advantages of seismic base isolation. Madhekar and Jangid (2011) used PFD in the benchmark highway bridge problem and found that the seismic response of the bridge can be controlled under near-fault motions. Zhang *et al.* (2012) performed an experimental study about the hysteretic performance of the pall-typed PFD and found, PFD had good force output capacity, and short response time and having the hysteretic behaviors are stable.

In modern highways, use of curved concrete bridges is increased for traffic separation structure, geological constraint and pleasant aesthetic view. Past seismic performance, indicated that the curved bridges may get to fail or damaged due to shear failure of piers and due to excessive displacement of bridge deck and bearings, due to unseating, pounding and the rotation of the superstructure or outward displacement (Galindo *et al.* 2009). During the San Fernando earthquake of 9 February 1971, the Northridge earthquake of 17 January 1994, and Wenchuan earthquake of 12 may 2008, some curved highway bridges suffered significant damage/collapsed (Williams and Godden, 1976; Fenves and Ellery, 1998; Galindo *et al.* 2009 and Liu and Wang 2014). Bridges play an important role during and after the seismic event by providing a way for accessing utilities, getting important things for survivable and provide to entry and exit route. Hence, bridges are lifeline structure and should withstand during the catastrophic seismic event. Kunde and Jangid (2003) recognized in their literature the use of a variety of passive isolation devices for seismic control of bridges by the number of researchers worldwide. The function of passive isolation technique is extremely efficient in controlling the seismic forces on the structure at the cost of increasing deck and bearing displacement. Excessive displacement of deck and the bearing may result into unseating at the bearing, hammering of deck and creating uncomfortable conditions for the traffic movement on deck. One of the ways to protect the bridge is to use the hybrid system consist of an isolation device with dampers.

Further, for seismic control of the curved bridge against dynamic loading some researcher perform the experimental and analytical studies. Lei and Chien (2004) in their study shown that, the isolation performance on base shear reduction of the curved bridge depends on the type of earthquake and angle of curvature of the structure. It was noted that the LRB with higher

flexibility or FPS with a lower frictional coefficient significantly reduces the base shear. Liu *et al.* (2011) established the three-dimensional computational model for a double-pier curved continuous girder bridge, and added viscous dampers at the positions of sliding bearings. Results show the viscous dampers can reduce the difference of internal force between the inner pier and outer pier in double-pier curved bridge, and it can effectively reduce the bending and twisting coupling effect of the curved bridge. Ates and Constantinou (2011a, b) found the effects of earthquakes on the response of the isolated and non-isolated curved bridges using response history analysis and response spectrum analysis including the effect of soil–structure interaction. It was found that the internal forces of the deck in the isolated curved bridge decrease compare with non-isolated. Recently, Monzon *et al.* (2012) studied experimentally the seismic response of full and hybrid isolated curved bridges and found both the techniques are successful at protecting the column.

From the review of literature, it is noted that there is no specific study so far had been carried out on application of semi-active PFD to the isolated curved bridge. Therefore, the aim of the present study is to investigate the effectiveness of hybrid semi-active systems for seismic response control of the curved concrete box girder bridge. The objectives of the study are summarized as, (i) to investigate the effectiveness of hybrid system PFD+LRB for seismic response control of the curved concrete box girder bridge problem, (ii) to investigate the influence of variation in important parameters of the damper on the response of the bridge and, (iii) to found the optimum value of the important parameters of the damper and (iv) to investigate the influence of passive and semi-active PFD on the response of the seismically isolated curved bridge.

2. Modelling of curved bridge

The bridge model considered for the present study is the design example no. 6 of "Federal Highway Administration (FHWA) Seismic Design Course", formulated   by BERGER/ABAM Engineers (Berger / Abam Engineers 1996), which was also studied by Ates and Constantinou (2011a, b). The bridge is having three spans, cast-in-situ concrete box girder supported over the reinforced concrete column as shown in Fig. 1. The span length of the bridge along the centerline is 27.25 m, 33.5 m, 27.25 m and width of the deck is 11.8m. The roadway alignment over the bridge is sharply horizontally curved (104°). The intermediate piers are made of rectangular cross-section having an area of 1.7 m^2 and 6.4 m height from the ground surface. The super structure consists of three-cell deck with 10% slope to the horizontal. The properties of the bridge system are same as considered in FHWA. It is assumed that the bridge is structurally safe (satisfying load and displacement demand) when the isolation device is introduced in between pier and superstructure. The deck is isolated from the supports by eight isolators (two at each pier cap and abutments), which are located at the corners of the cap. The material and geometrical properties of the considered curved bridge are given in Table 1. The following assumptions are considered for seismic analysis of the bridge.

- The deck and piers of the bridge system will remain in the elastic state under the action of dynamic loading.
- The abutments of the bridge are rigid and piers are fixed at the ground level.
- The soil structure interaction is ignored for the analysis.
- The deck of the bridge is modelled as a spine beam, which is made with small straight two node beam elements having six degree of freedom at each node.

- The mass of each element is distributed between the two adjacent nodes in the form of lumped mass.
- The stiffness of non-structural elements (sidewalk and parapet) are neglected.
- The bridge is subjected to horizontal and vertical components of earthquake ground motion.

Fig. 2 shows the idealized mathematical model of the curved bridge. The selected bridge is modelled as a multi-degrees-of-freedom (MDOF) system. Based on the detailed drawings of the curved bridge, a 3D evaluation model is made in MATLAB. The number of elements considered in the bridge deck and piers are 32 and 4, respectively.
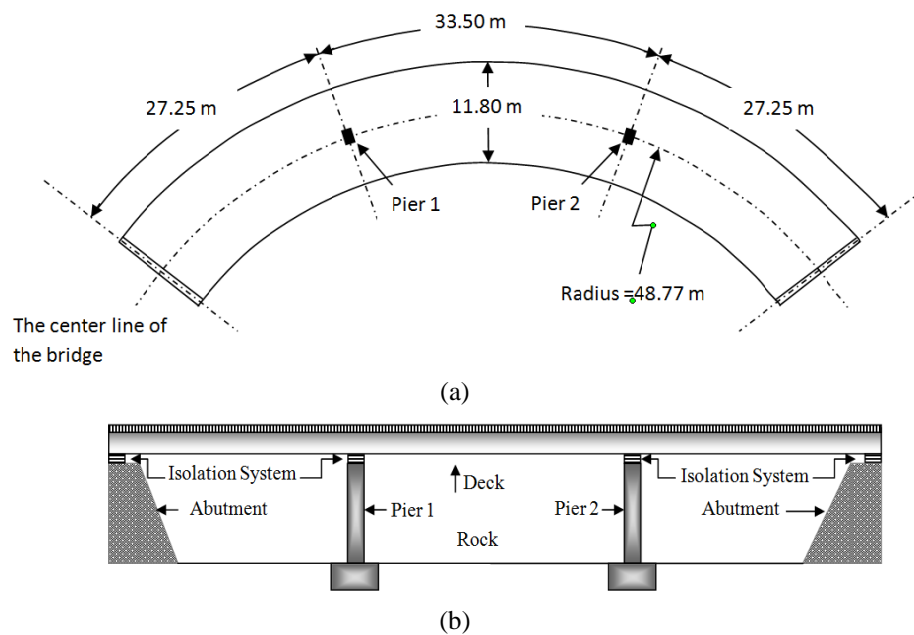

(a)

(b)

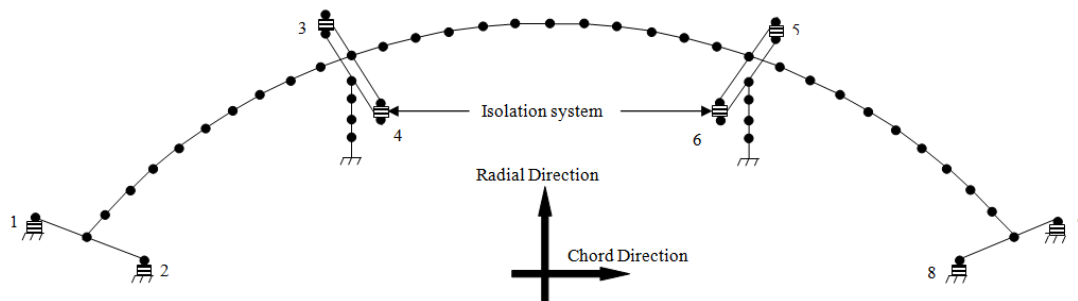Fig. 1 (a) The curved bridge plan, and (b) developed elevation

Fig. 2 Mathematical model of isolated bridge

Table 1 Properties of bridge deck and piers

Properties	Deck	Piers
Cross-sectional area (m2)	6.238	1.7
Moment of Inertia (m4)	2.7074	0.409416
Young's modulus of elasticity (N/m2)	3.2x1010	3.2x1010
Mass Density (kg/m3)	2.5x103	2.5x103
Length/height (m)	88	6.4

3. Governing equations of motion

The equations of motion for the curved bridge system subjected to seismic excitation are expressed in the matrix form as

$$[M]\{\ddot{u}(t)\} + [C]\{\dot{u}(t)\} + [K]\{u(t)\} = -[M][\eta]\{\ddot{u}_g(t)\} + [b]\{F(t)\} \tag{1}$$

$$\{u(t)\} = \{x_1, y_1, z_1, x_2, y_2, z_2 \dots \dots \dots, x_N, y_N, z_N\}^T \tag{2}$$

$$\{\ddot{u}_g(t)\} = \begin{Bmatrix} \ddot{x}_g(t) \\ \ddot{y}_g(t) \\ \ddot{z}_g(t) \end{Bmatrix} \tag{3}$$

where $[M]$, $[C]$, and $[K]$ are the mass, damping and stiffness matrices respectively; $\{\ddot{u}(t)\}, \{\dot{u}(t)\}$ and $\{u(t)\}$ are structural acceleration, structural velocity and structural displacement vector respectively; $\{F(t)\}$ is the vector of control force inputs, $\{\ddot{u}_g(t)\}$ is the vector of earthquake ground acceleration acting in three directions (i.e. two horizontal and one vertical); $\ddot{x}_g(t)$, $\ddot{x}_g(t)$ and $\ddot{z}_g(t)$ represent the earthquake ground acceleration (m/s^2) in chord, vertical and radial direction respectively; $[\eta]$ is an influence coefficient matrix, relating the ground acceleration to the bridge degrees-of-freedom (DOF); and $[b]$ is an matrix relating the forces produced by the control devices to the bridge DOF.

Firstly, individual elemental stiffness matrix of each element with six DOF at each node using beam element is formed and using a transformation matrix, it is converted into the global elemental matrix. A global structural stiffness matrix is assembled using elemental global stiffness matrices. Similarly, the global mass matrix for the curved bridge is assembled. Then structural stiffness matrix for numerical integration is obtained by dynamic condensation from the global structural stiffness matrix. The global damping matrix is a combination of the distributed 5% inherent Rayleigh damping in the first two modes. Consequently, the response of the curved bridge is evaluated step-by-step at successive increments of time using Newmark-beta method. It is assumed that the properties of the bridge system remain constant during the time increment.

4. Modelling of isolation system and damper

The restoring force generated by the device depends on the characteristic of isolator and damper considered. For present study lead rubber bearing (LRB) and piezoelectric friction damper (PFD) are considered. The detail of modelling of each device is keyed out as below.

4.1 Lead rubber bearing

LRB is one type of the elastomeric bearing consists of thin layers of steel and high damping rubber plates built in alternate layers with a lead plug at its center as shown in Fig. 3(a). The LRB was invented in New Zealand in 1975 (Robinson and Tucker 1977) and has been widely used in New Zealand and other nations. This bearing provides a vertical support and horizontal flexibility, and energy absorbing capacity (Robinson 1982). In addition, LRB can safely tolerate strain up to 200% for the occasional very large earthquakes (Tyler and Robinson 1984). The interlocked steel plates in the bearing, forces the lead core to deform its entire volume in pure shear. From past test and theory analysis, it is observed that the force deformation behavior of the LRB is nonlinear in nature. In the present study, Wen's model (Wen 1976) is used to characterize the hysteretic behavior of the LRB, which is shown schematically in the Fig. 3(b). The restoring force developed in the isolation bearing is given by

$$F_x = c_b \dot{x}_b + \alpha k_b x_b + (1 - \alpha) f_0 Z_x \tag{4}$$

$$F_y = c_b \dot{y}_b + \alpha k_b y_b + (1 - \alpha) f_0 Z_y \tag{5}$$

where k_b, c_b are the initial stiffness and viscous damping of the bearing; f_0 is the yield strength of the bearing; α is an index which represent the ratio of post-to pre-yielding stiffness; and Z_x and Z_y are hysteretic dimensionless displacement components governed by Wen's model. In the present study, these components are considered to satisfying the following bi-directional interaction nonlinear first-order differential equation (Park *et al.* 1986).

$$q \begin{Bmatrix} \dot{Z}_x \\ \dot{Z}_y \end{Bmatrix} = \begin{bmatrix} A - \beta sign(\dot{x}_b)|Z_x|Z_x - \tau Z_x^2 & -\beta sign(\dot{y}_b)|Z_y|Z_x - \tau Z_x Z_y \\ -\beta sign(\dot{x}_b)|Z_x|Z_y - \tau Z_x Z_y & A - \beta sign(\dot{y}_b)|Z_y|Z_x - \tau Z_y^2 \end{bmatrix} \begin{Bmatrix} \dot{x}_b \\ \dot{y}_b \end{Bmatrix} \tag{6}$$

where q is the yield displacement; β, τ and A are dimensionless parameter such that predict response from the model closely matches the experimental results. In the present study the value of parameter are q=25 mm, A=1, β=0.5 and τ =0.5 considered for LRB. The LRB system is mainly characterized by the isolation period (T_b), damping ratio (ξ_b) and normalized yield strength (F_0). The bearing parameters T_b, ξ_b and are F_0 computed by Eq. (7). In the present study, the damping ratio equals to 0.05 is considered.

$$T_b = 2\pi \sqrt{\frac{M}{k_b}}, \qquad \xi_b = \frac{c_b}{2M\omega_b} \text{and} \quad F_0 = \frac{\sum f_0}{W} \tag{7}$$

where, M is the total mass of the bridge deck; and $\omega_b = 2\pi/T_b$ is the isolation frequency, W is the total weight of deck.

4.2 Modelling of piezoelectric friction damper

Figure 4 shows the schematic diagram of a friction damper. It consists of two U-shaped bodies sliding on each other with piezoelectric stack actuators inside the internal body. The contact clamping force applied to the damper $N(t)$ is controllable. The friction damper generates a dissipative friction force proportional to the coefficient of friction between the two bodies and contact force. The dynamic behaviour of the friction dampers is improved by controlling the

contact clamping force based on the feedback of the damper slippage using piezoelectric stack actuators. The contact clamping force on two friction surfaces can be synchronized accordingly as per requirement by electrifying the piezoelectric stack materials. Chen and Chen (2000, 2004) proposed semi-active control algorithm to regulate the clamping force of the PFD. The algorithm consists of a passive damping mechanism, and the active counterpart. When the structure experiences high-amplitude vibrations, the active mechanism is triggered where as low–amplitude vibrations are controlled by passive coulomb damping. The control algorithm takes into account the both stick and sliding phases. The main aim of PFD is to increase the damping of structure, without changing the structural stiffness. In order to control the seismic response of structure, a simple semi-active control algorithm for PFD proposed by Chen and Chen (2002) is used. A PFD changes the normal force exerted on the vibrating structure as

$$N_i(t) = \begin{cases} N_{pre} & when\ e|u_i(t)| + g|\dot{u}_i(t)| \le N_{pre} \\ e|u_i(t)| + g|\dot{u}_i(t)| & when\ e|u_i(t)| + g|\dot{u}_i(t)| > N_{pre} \end{cases} \tag{8}$$

where N_{pre} is the required pre-load on the multilayered stack actuators to generate required passive force; e (kN/m) and g (kNs/m) are positive gain factors of displacement and velocity respectively; $|\dot{u}_i(t)|$ and $|u_i(t)|$ are the absolute values of relative velocity and displacement of the ith damper respectively. In Eq. (8) first expression represent the passive coulomb damper mechanism of the semi-active control algorithm, when the structural responses are relatively small. The active damper mechanism represented by the second part is activated only under high amplitude excitations. The friction force of the ith damper $f_i(t)$ is given by

$$f_i(t) = 2\mu_d N_i(t) sgn[\dot{u}_i(t)] \tag{9}$$

where, μ_d is the coefficient of friction and factor 2 is used to account for two friction surface. From Eqs. (8) and (9) $f_i(t)$ is given by

$$f_i(t) = \begin{cases} 2\mu_d N_{pre} sgn[\dot{u}_i(t)] & when\ e|u_i(t)| + g|\dot{u}_i(t)| \le N_{pre} \\ 2\mu_d[e|u_i(t)| + g|\dot{u}_i(t)|] & when\ e|u_i(t)| + g|\dot{u}_i(t)| > N_{pre} \end{cases} \tag{10}$$

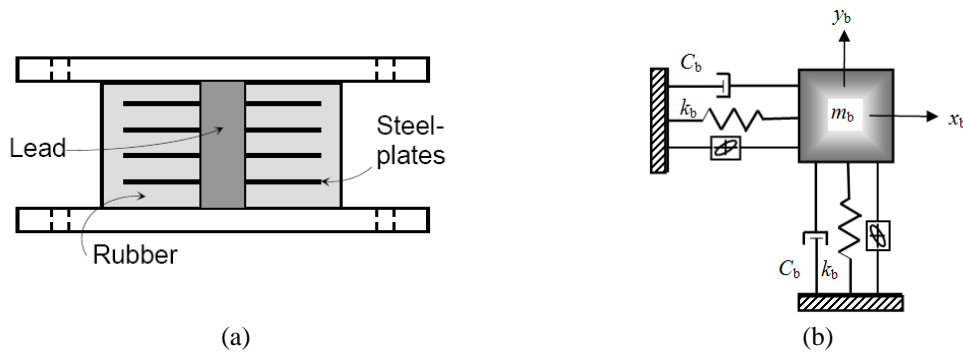(a)   (b)

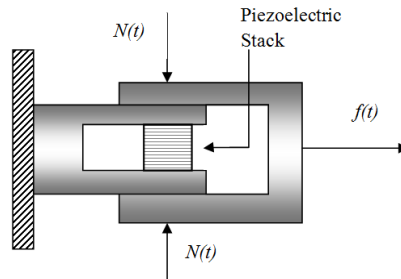Fig. 3 (a) Lead Rubber Bearing (LRB) and (b) schematic diagram

Fig. 4 Piezoelectric friction damper (PFD)

The semi-active control strategy of PFD is mainly depending on the four factors as coefficient of friction (μ_d), gain factors of displacement (e), gain factors of velocity (g) and pre-load N_{pre}. For the application to the curved bridge, the semi-active control strategy is implemented and 8 PFD are used, 4 in chord direction and 4 in the radial direction. These PFD are placed above the pier cap and below the deck, and at the abutment location.

5. Numerical study

The structural model of the isolated curved box girder bridge with PFD developed in MATLAB, and seismic time history analysis are carried out. For the analysis, four real earthquakes ground motion namely; El Centro (1940), Northridge (1994), Loma prieta (1989) and Kobe (1995) earthquakes with all three components are considered. Table 2 presents the important feature of all considered ground motions. In the analysis, all the ground motions are used with the full strength with the east-west and the north-south components are applied in the chord and radial direction of the bridge, respectively. The present numerical study focused on the effect of variation of important parameter mainly coefficient of friction, gain factors of displacement, gain factors of velocity and pre-load of the PFD on the performance of the curved bridge in order to identify the optimum value of parameters. Considering the values of important parameters of isolators constant as for the LRB Fo= 0.1 and the isolation period equal to 2 sec throughout the analysis.

In order to evaluate performance a set of performance evaluation criteria were considered. The evaluation criteria J_1 to J_4 are described to measure the reduction in peak base shear, peak overturning moment, peak mid-span displacement and peak mid-span acceleration of the curved box girder bridge. These measures are calculated by normalizing the peak response quantities of the controlled bridge by the corresponding peak response quantities for the uncontrolled bridge (with rigid deck to pier connection); J_6 to J_9 are described to measure the reduction in norm base shear, norm overturning moment, norm mid-span displacement and norm mid-span acceleration of the curved box girder bridge. These measures calculated by normalizing the norm response quantities by the corresponding norm response of the uncontrolled bridge. J_5 and J_{10} are associated to the peak and the norm displacement of the bearing and obtained by calculating relative displacement of bearing end. J_{11} is related to the peak control force generated by the device normalized by the seismic weight of the bridge.

Table 2 Earthquake data for numerical simulation

Earthquake	Recording Station	Duration (s)	PGA (g)		
			Vertical	N-S	E-W
El Centro (1940)	117 El Centro Array #9	40	0.205	0.313	0.215
Loma Prieta (1989)	16 LGPC	24.965	0.89	0.563	0.605
Northridge (1994)	24514 Sylmar - Olive View Med FF	40	0.535	0.834	0.604
Kobe (1995)	KJMA	48	0.343	0.821	0.599

5.1 Semi-active control of PFD

To investigate the robustness of the hybrid system on the seismic response of the curved box girder bridge, the responses are obtained by varying important parameters of the PFD. Initially, coefficient of friction μ_d is varied from 0.02 to 0.2, and keeping other variables constant as g =1000kNs/m, e/g=3 and N_{pre} as 10% of the capacity of damper, i.e. 100 kN.

The variation of evaluation criteria for peak base shear, peak overturning moment, peak mid-span displacement, peak mid-span acceleration, peak displacement of bearing and peak control force for different μ_d value of PFD+LRB combination are shown in Fig. 5 and 6. It is observed that, (i) the base shear and overturning moment at the base of the pier decreases/increases slightly by increasing μ_d as per earthquake characteristics, (ii) the mid-span displacement and bearing displacement decreases with increasing μ_d, (iii) the mid-span acceleration remain constant with increasing μ_d and (iv) the peak control force gets increased by increasing μ_d for all considered earthquakes in the chord and radial direction. These variations are due to, increase in μ_d, results in the increasing frictional force and decreasing relative displacement across the damper. Considering the value for μ_d as 0.1, significant reduction in all responses for all considered earthquakes is achieved and this can be taken as an optimum value.
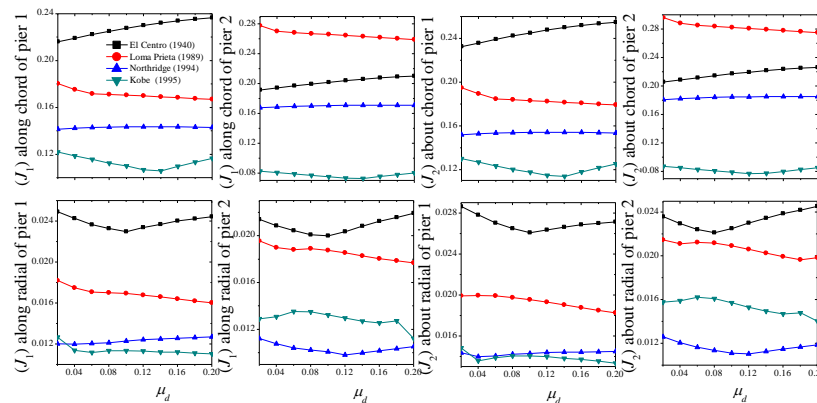

Fig. 5 Effect of coefficient of friction (μ_d) of PFD on peak base shear (J_1) and peak overturning moment (J_2)
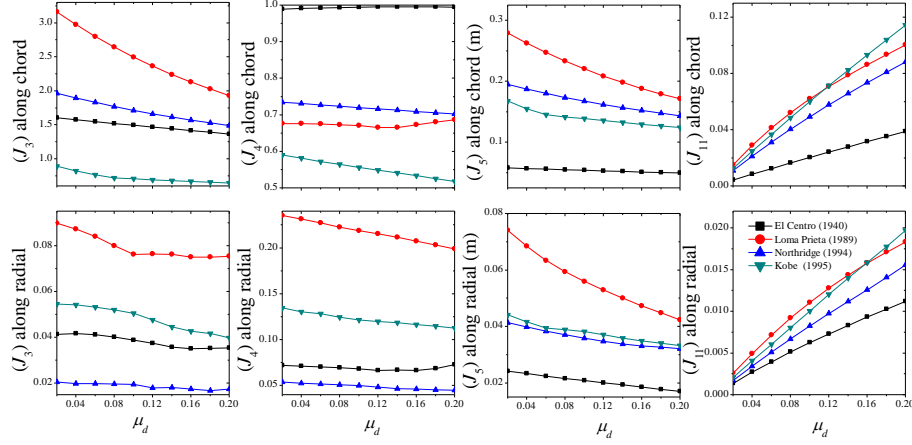
Fig. 6 Effect of coefficient of friction (μ_d) of PFD on peak mid span displacement (J_3), peak mid span acceleration (J_4), peak displacement of bearing (J_5) and peak control force (J_{11})
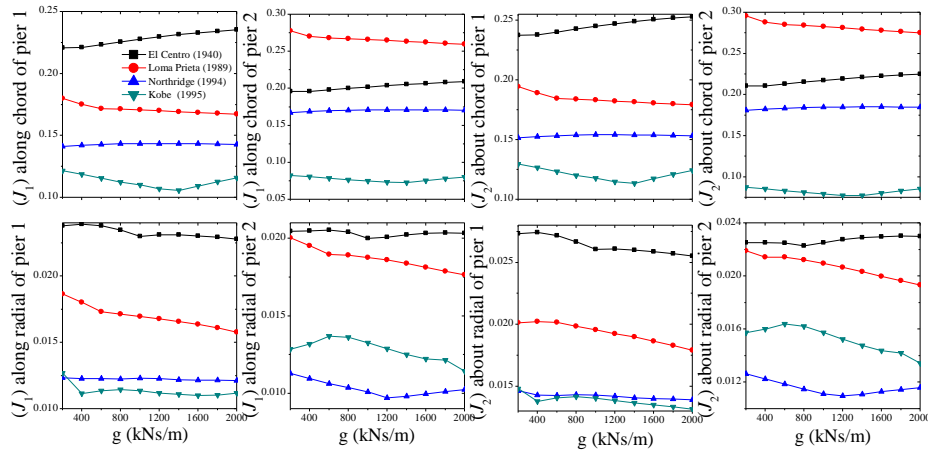

Fig. 7 Effect of gain factor (g) of PFD on peak base shear (J_1) and peak overturning moment (J_2)

Further, the velocity gain factors (g) is varied from 200 kNs/m to 2000 kNs/m, and keeping other variables as constant as μ_d=0.1, e/g=3 and N_{pre}=100 kN. Figs. 7 and 8 show variations of evaluation criteria for the different g values. It is observed that,

(i) the base shear and overturning moment at the base of the pier slightly decreases/increases by increasing g in as per the considered earthquake, (ii) the mid-span displacement and bearing displacement decreases with increasing g, (iii) the mid-span acceleration slightly decreases with increasing g and (iv) the peak control force get increased by increasing g for all considered earthquake in the chord and radial direction. These variations are due to, increase in g results in the increasing normal force acting on the damper.
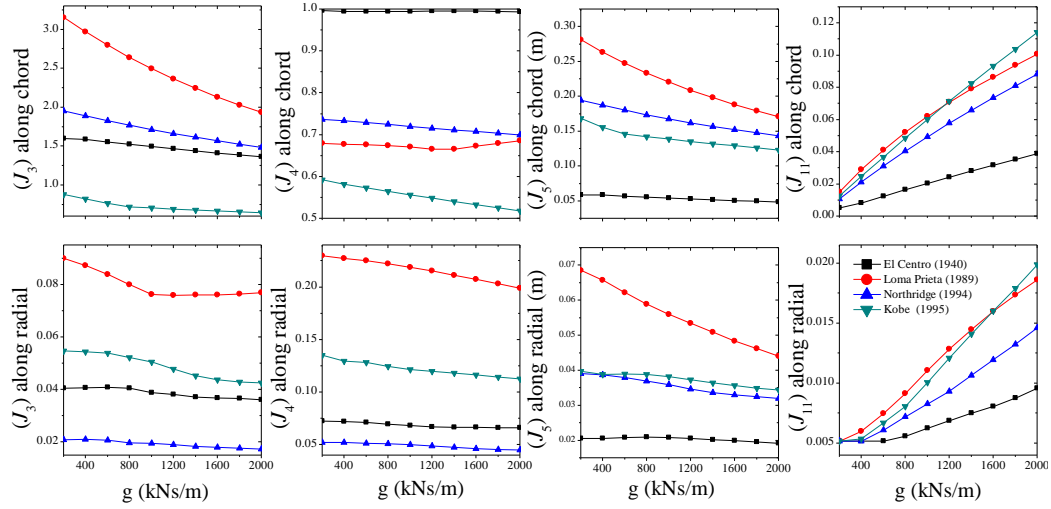
Fig. 8 Effect of gain factor (g) of PFD on peak mid span displacement (J_3), peak mid span acceleration (J_4), peak displacement of bearing (J_5) and peak control force (J_{11})
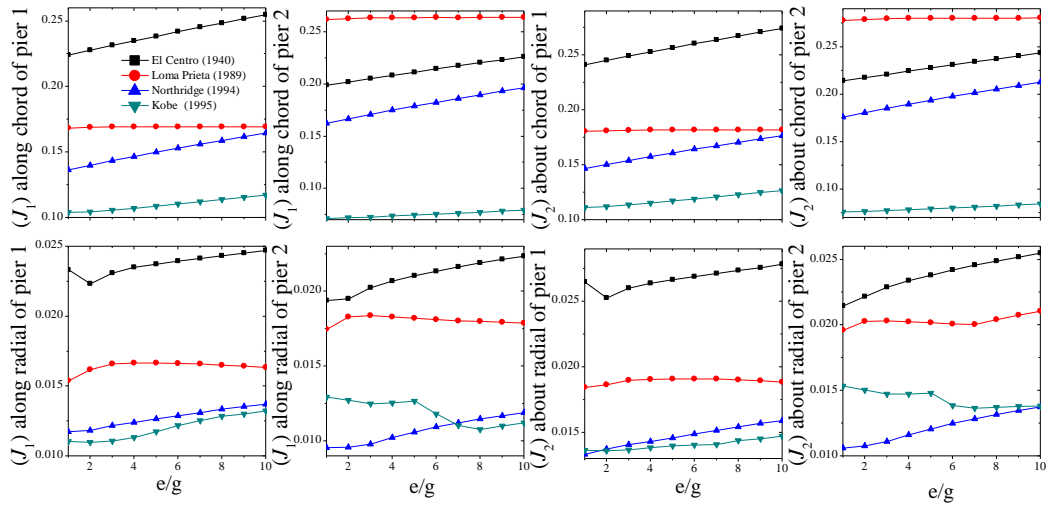

Fig. 9 Effect of gain ratio (e/g) of PFD on peak base shear (J_1) and peak overturning moment (J_2)

From plots, it is observed that higher value of a gain factor of velocity is beneficial to reduce the mid-span displacement and bearing displacement. Therefore, considering the optimum value of g as 1400 kNs/m for a better response of peak mid-span displacement and bearing displacement on the cost of slightly increase in peak base shear and overturning moment for the VFD+LRB.
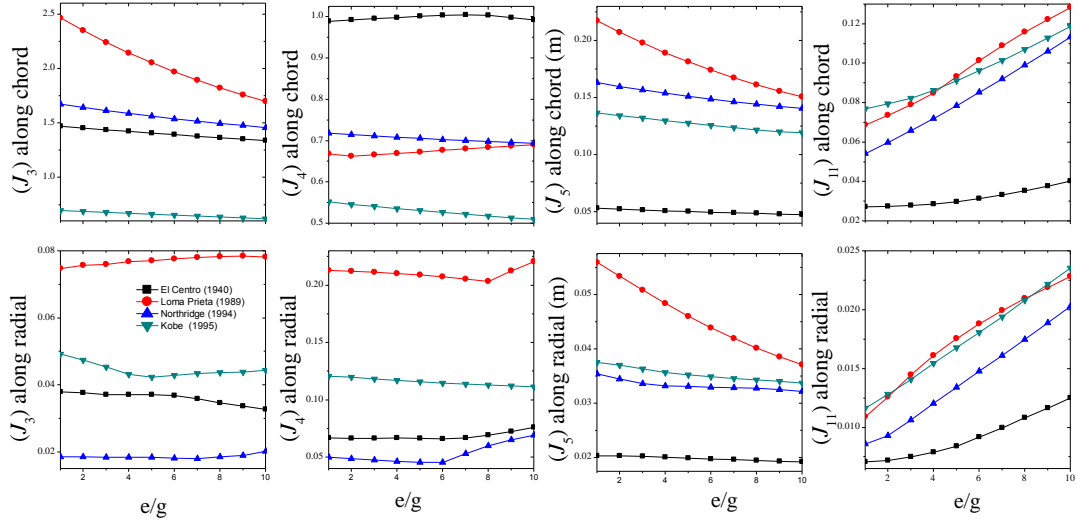
Fig. 10 Effect of gain ratio (e/g) of PFD on peak mid span displacement (J_3), on peak mid span acceleration (J_4), peak displacement of bearing (J_5) and peak control force (J_{11})
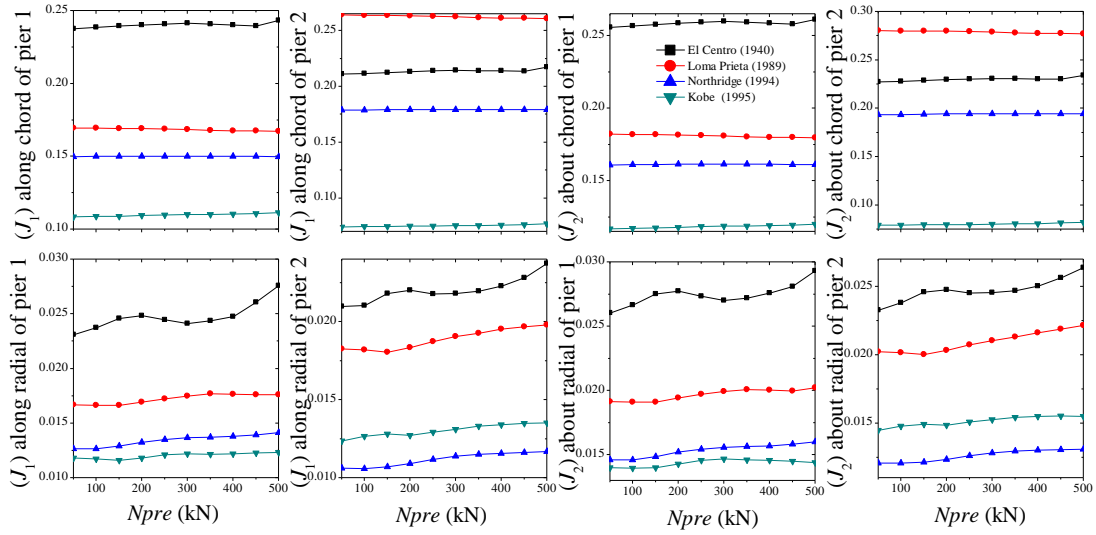

Fig. 11 Effect of N_{pre} of PFD on peak base shear (J_1) and peak overturning moment (J_2)

Further, instead of varying gain factors (e) the ratio e/g is varied from 1 to 10, and keeping other variable as constant as μ_d=0.1, g=1400 kNs/m and N_{pre}=100 kN. The variation of evaluation criteria for different e/g values of PFD are shown in Fig. 9 and 10.
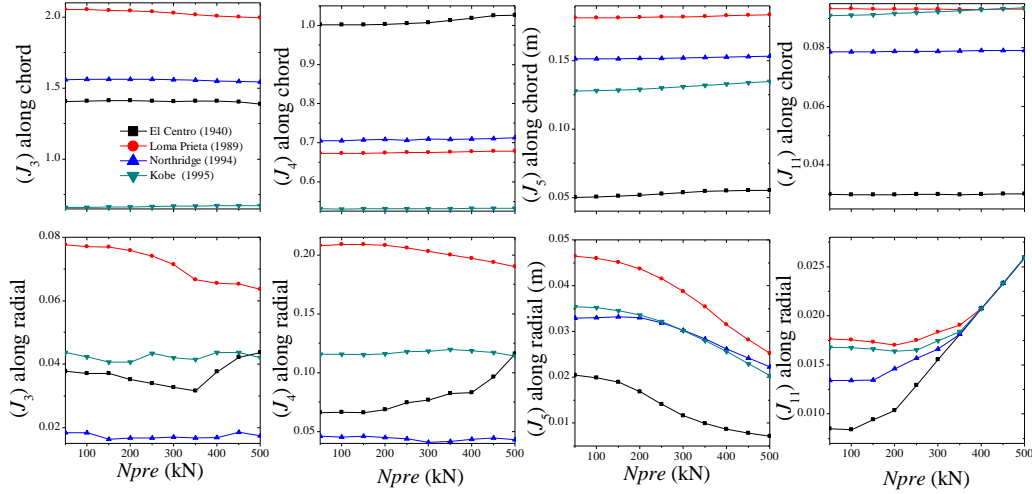
Fig. 12 Effect of N_{pre} of PFD on peak mid span displacement (J_3), on peak mid span acceleration (J_4), peak displacement of bearing (J_5) and peak control force (J_{11})
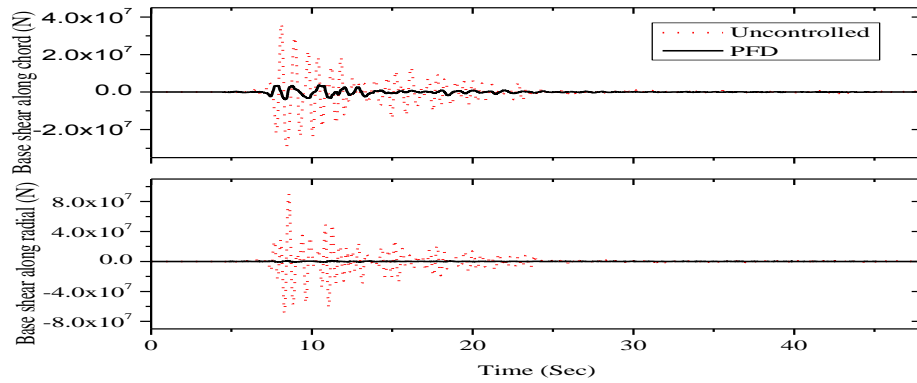

Fig. 13 Time variation of base shear of pier 1 along the chord and radial direction of bridge under Kobe (1995) earthquake

It is observed that, (i) the base shear and overturning moment at the base of the pier increase slightly by increasing e/g, (ii) the mid-span displacement and bearing displacement decreases with increasing e/g, (iii) the mid-span acceleration slightly decreases with increasing e/g and (iv) the peak control force get increased by increasing e/g for all considered earthquake in the chord and radial direction. These variations are due to, increase in e/g results in the increasing normal force acting on the damper. From plots in all combinations, it is observed that higher value of a gain ratio is beneficial to reduce the mid-span displacement and bearing displacement and lower value for base shear and overturning moment. Therefore, considering the optimum value of e/g as 5 for a better response of bridge.

Table 3 Evaluation criteria J_1 to J_4 and J_6 to J_9

Earthquake			El Centro (1940)		Loma Prieta (1989)		Northridge (1994)		Kobe (1995)	
Peak Value	Location		Passive	Semi-active	Passive	Semi-active	Passive	Semi-active	Passive	Semi-active
J_1	Pier 1	Chord	0.22	0.24	0.18	0.17	0.14	0.15	0.12	0.11
		Radial	0.02	0.02	0.02	0.02	0.01	0.01	0.01	0.01
	Pier 2	Chord	0.20	0.21	0.28	0.26	0.17	0.18	0.08	0.07
		Radial	0.02	0.02	0.02	0.02	0.01	0.01	0.01	0.01
J_2	Pier 1	Chord	0.24	0.26	0.20	0.18	0.15	0.16	0.13	0.12
		Radial	0.03	0.03	0.02	0.02	0.01	0.01	0.02	0.01
	Pier 2	Chord	0.21	0.23	0.30	0.28	0.18	0.19	0.09	0.08
		Radial	0.02	0.02	0.02	0.02	0.01	0.01	0.02	0.01
J_3	Deck	Chord	1.60	1.41	3.25	2.05	1.98	1.56	0.90	0.66
		Radial	0.04	0.04	0.09	0.08	0.02	0.02	0.05	0.04
		Vertical	1.82	1.83	3.29	3.29	0.83	0.83	2.07	2.08
J_4	Deck	Chord	1.00	1.00	0.68	0.67	0.74	0.71	0.60	0.53
		Radial	0.07	0.07	0.23	0.21	0.05	0.05	0.14	0.12
		Vertical	0.57	0.57	0.93	0.93	0.53	0.53	1.19	1.19
J_6	Pier 1	Chord	0.27	0.26	0.24	0.23	0.19	0.18	0.15	0.15
		Radial	0.03	0.03	0.02	0.02	0.02	0.01	0.02	0.01
	Pier 2	Chord	0.25	0.24	0.25	0.25	0.20	0.18	0.13	0.13
		Radial	0.02	0.02	0.02	0.02	0.02	0.01	0.01	0.01
J_7	Pier 1	Chord	0.29	0.28	0.25	0.25	0.20	0.19	0.16	0.16
		Radial	0.03	0.03	0.02	0.02	0.02	0.02	0.02	0.02
	Pier 2	Chord	0.27	0.26	0.27	0.26	0.21	0.20	0.14	0.14
		Radial	0.03	0.03	0.03	0.03	0.02	0.02	0.02	0.01
J_8	Deck	Chord	1.60	1.42	2.50	1.90	1.86	1.45	1.21	0.95
		Radial	0.03	0.03	0.08	0.07	0.03	0.03	0.04	0.03
		Vertical	1.83	1.84	3.33	3.34	1.77	1.77	2.39	2.39
J_9	Deck	Chord	0.84	0.81	0.77	0.73	0.56	0.53	0.58	0.55
		Radial	0.07	0.07	0.21	0.19	0.06	0.06	0.10	0.09
		Vertical	0.85	0.85	1.55	1.55	0.82	0.82	1.32	1.32
J_{11}	Bridge	Chord	0.01	0.03	0.01	0.09	0.01	0.08	0.01	0.09
		Radial	0.01	0.01	0.01	0.02	0.01	0.01	0.01	0.02

Table 4 Evaluation criteria J_5 and J_{10}

| Control Type			El Centro (1940)		Loma Prieta (1989)		Northridge (1994)		Kobe (1995)	
Peak Value	Location		Passive	Semi-active	Passive	Semi-active	Passive	Semi-active	Passive	Semi-active
J_5(m)	B - 1	Chord	0.06	0.05	0.29	0.18	0.20	0.15	0.17	0.13
		Radial	0.02	0.02	0.07	0.05	0.04	0.03	0.04	0.04
	B - 2	Chord	0.06	0.05	0.28	0.18	0.19	0.15	0.17	0.12
		Radial	0.02	0.02	0.06	0.04	0.03	0.03	0.03	0.03
	B - 3	Chord	0.06	0.05	0.28	0.17	0.19	0.14	0.17	0.12
		Radial	0.01	0.01	0.03	0.02	0.01	0.01	0.02	0.02
	B - 4	Chord	0.05	0.05	0.28	0.17	0.19	0.14	0.17	0.12
		Radial	0.01	0.01	0.02	0.02	0.01	0.01	0.02	0.02
	B - 5	Chord	0.06	0.05	0.28	0.17	0.19	0.14	0.17	0.12
		Radial	0.01	0.01	0.03	0.02	0.01	0.01	0.02	0.02
	B - 6	Chord	0.05	0.05	0.28	0.17	0.19	0.14	0.17	0.12
		Radial	0.01	0.01	0.02	0.01	0.01	0.01	0.01	0.01
	B - 7	Chord	0.06	0.05	0.29	0.18	0.20	0.15	0.17	0.13
		Radial	0.02	0.02	0.07	0.04	0.04	0.04	0.04	0.03
	B - 8	Chord	0.06	0.05	0.29	0.18	0.19	0.15	0.17	0.12
		Radial	0.02	0.02	0.06	0.04	0.03	0.03	0.03	0.03
J_{10}	B - 1	Chord	0.01	0.01	0.06	0.05	0.03	0.02	0.03	0.03
		Radial	0.01	0.00	0.01	0.01	0.01	0.01	0.01	0.01
	B - 2	Chord	0.01	0.01	0.06	0.05	0.03	0.02	0.03	0.03
		Radial	0.00	0.00	0.01	0.01	0.00	0.00	0.01	0.01
	B - 3	Chord	0.01	0.01	0.06	0.05	0.03	0.02	0.03	0.02
		Radial	0.00	0.00	0.00	0.00	0.00	0.00	0.00	0.00
	B - 4	Chord	0.01	0.01	0.06	0.05	0.03	0.02	0.03	0.02
		Radial	0.00	0.00	0.00	0.00	0.00	0.00	0.00	0.00
	B - 5	Chord	0.01	0.01	0.06	0.05	0.03	0.02	0.03	0.02
		Radial	0.00	0.00	0.00	0.00	0.00	0.00	0.00	0.00
	B - 6	Chord	0.01	0.01	0.06	0.05	0.03	0.02	0.03	0.02
		Radial	0.00	0.00	0.00	0.00	0.00	0.00	0.00	0.00
	B - 7	Chord	0.01	0.01	0.06	0.05	0.03	0.02	0.03	0.03
		Radial	0.01	0.00	0.01	0.01	0.01	0.01	0.01	0.01
	B - 8	Chord	0.01	0.01	0.06	0.05	0.03	0.02	0.03	0.03
		Radial	0.00	0.00	0.01	0.01	0.00	0.00	0.01	0.01
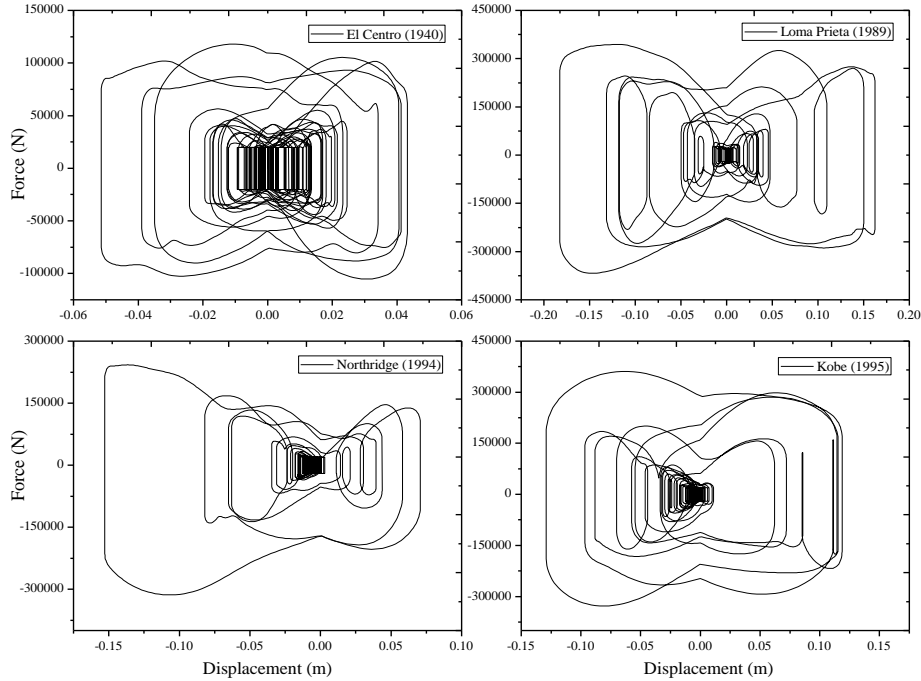
Fig. 14 Force-displacement behaviour of PFD (D1) with semi-active control under different Earthquake motion

Further, pre-load N_{pre} is varied from 50 kN to 500 kN, and keeping other variables as constant as $\mu_d = 0.1$, $g = 1400$ kNs/m and $e/g=5$. The variation of evaluation criteria for different N_{pre} values of PFD are shown in Fig. 11 and 12. It is observed that evaluation criteria are not significantly influenced by the variation in N_{pre} in chord direction, whereas slightly changes in radial direction for different value. To maintain the effectiveness of PFD, N_{pre} is kept as 100 kN.

Considering the value of the $\mu_d=0.1$, $g = 1400$ kNs/m, $e/g = 5$ and $N_{pre}=100$ kN of PFD as an overall better response control for PFD+LRB hybrid system. Table 3 and 4 shows the values of different evaluation criteria for all earthquakes. From table 3 and 4 it is observed that, maximum reduction in base shear and overturning moment is observed under Kobe earthquake among the all considered earthquakes; the considered combination of PFD+LRB is effective in controlling the base shear, overturning moment, mid-span displacement, mid-span acceleration and bearing displacement. Fig. 13 shows the results of time history analysis along the chord and radial direction for reduction in base shear of pier 1 under the Kobe (1995) earthquake for PFD+LRB combination. From the figure, it is observed that due to use of the PFD+LRB huge amount of reduction in base shear in the chord and radial direction of the pier occur compared to uncontrolled structure. The force-displacement variation loops at D1 (damper 1 in chord direction at left abutment) for the curved bridge system under the different time histories for semi-active control law are shown in Fig. 14. It is observed from the hysteresis loops that considerable amount of energy is absorbed by the PFD under all the time histories.

5.2 Passive control of PFD

In order to compare the semi-active response of PFD, response of the curved bridge with passive PFD is evaluated with parameter μ_d=0.1 and N_{pre}=100 kN. Table 3 and 4 shows the values of different evaluation criteria for all earthquakes under passive and semi-active cases. From the table, it is clear that semi-active control system is much more useful to control the mid-span displacement, mid-span acceleration and bearing displacement compare with passive control strategy of PFD. This reduction in mid-span displacement, mid-span acceleration and bearing displacement can be achieved with slightly increase in base shear and overturning moment using semi-active hybrid system.

6. Conclusions

The seismic response of the horizontally curved concrete box girder bridge isolated with lead rubber bearing and equipped with smart material damper, piezoelectric friction damper for the different control strategies investigated. The effectiveness of the PFD is studied by varying important parameters for assessment of its performance for different earthquake ground motions. Based on the investigation carried out, the following conclusions have been drawn:

1) Use of piezoelectric smart material in the friction damper enhances the capability of the damper and makes smoothen functioning by utilizing less power in seismic control.
2) Significant seismic response reduction of the curved bridge can be achieved by applying hybrid control system consisting of LRB with PFD.
3) The reduction of the seismic responses depends on the earthquake ground motions.
4) The higher value of a coefficient of friction, gain factor *g* and gain ratio *e/g* will be beneficial for lower mid-span displacement and bearing displacement.
5) The variation in pre-load of PFD is not significantly influenced the response of the curved bridge.
6) The semi-active control strategy of PFD is highly effective for controlling the mid-span displacement; mid-span acceleration and bearing displacement as compared with a passive control strategy at the cost of slightly increase in base shear and moment.

References

Ates, S. and Constantinou, M.C. (2011a), "Example of application of response history analysis for seismically isolated curved bridges on drilled shaft with springs representing soil", *Soil Dyn. Earthq. Eng.*, **31**, 334-350.

Ates, S. and Constantinou, M.C. (2011b), "Example of application of response spectrum analysis for seismically isolated curved bridges including soil-foundation effects", *Soil Dyn. Earthq. Eng.*, **31**, 648-661.

Berger/Abam Engineers, (1996), Federal Highway Administration Seismic Design Course, Design Example No. 6, Publication no. FHWA-SA-97-011 and Barcode no. PB97-142111.

Chen, G.D. and Chen, C.C. (2000), "Behavior of piezoelectric friction dampers under dynamic loading", *Proceedings of the SPIE Symposium on Smart Structure Materials, Smart Systems for Bridges, Structures, and Highways*, Newport Beach, California, April.

Chen, C. and Chen, G. (2002), "Non-linear control of a 20-storey steel building with active piezoelectric

friction dampers", *Struct. Eng. Mech.*, **14**(1), 21-38.

Chen, G. and Chen, C. (2004), "Semi-active control of the 20-story benchmark building with piezoelectric friction dampers", *J. Eng. Mech. - ASCE*, **130**(4), 393-400.

Monzon, E.V., Wei, C., Buckle, I.G. and Itani A. (2012), "Seismic response of full and hybrid isolated curved bridges", *Structures Congress,* Chicago, Illinois, March.

Fenves, G.L. and Ellery, M. (1998), "Behavior and failure analysis of a multiple-frame highway bridge in the 1994 northridge earthquake", *Pacific Earthquake Engineering Research Center*, Report No. PEER 98/08, University of California, Berkeley, California.

Galindo, C.M., Hayashikawa, T. and Belda, J.G. (2009), "Damage evaluation of curved steel bridges upgraded with isolation bearings and unseating prevention cable restrainers", *World Acad. Sci. Eng. Tech.*, **59**, 53-61.

Kunde, M.C. and Jangid, R.S. (2003), "Seismic behavior of isolated bridges: A-state-of-the-art review", *Elect. J. Struct. Eng.*, **3**(3), 140-170.

Lei, Y.H. and Chien, Y.L. (2004), "Applications of LRB and FPS to 3-D curved box bridges", *Tamkang J. Sci. Eng.*, **7**(1), 17-28.

Liu, K. and Wang, L.H. (2014), "Earthquake damage of curved highway bridges in 2008 wenchuan earthquake", *Adv. Mat. Res.*, **838-841**, 1571-1576.

Liu, Y., Qi, X., Wang, Y. and Chen, S. (2011), "Seismic mitigation analysis of viscous dampers for curved continuous girder bridge", *Appl. Mech. Mat.*, **90-93**, 1230-1233.

Madhekar, S.N. and Jangid, R.S. (2011), "Seismic performance of benchmark highway bridge installed with piezoelectric friction dampers", *The IES J. Part A: Civil Struct. Eng.*, **4**(4), 191-212.

Ozbulut, O.E. and Hurlebaus, S. (2010), "Fuzzy control of piezoelectric friction dampers for seismic protection of smart base isolated buildings", *Bull. Earthq. Eng.*, **8**, 1435–1455.

Park, Y.J., Wen, Y.K. and Ang, A.H.S. (1986), "Random vibration of hysteretic systems under bi-directional ground motions", *Earthq. Eng. Struct. D.*, **14**(4), 543-557.

Robinson, W.H. (1982), "Lead-rubber hysteretic bearings suitable for protecting structures during earthquakes", *Earthq. Eng. Struct. D.*, **10**, 593-604.

Robinson, W.H. and Tucker, A.G. (1977), "A lead -rubber shear damper", *Bull. NZ Soc. Earthquake Eng.*, **10**(3), 151-153.

Tyler, R.G. and Robinson, W.H. (1984), "High-strain tests on lead-rubber bearings for earthquake loadings", *Bull. NZ Soc. Earthq. Eng.*, **17**(2), 90-105.

Wen, Y.K. (1976), "Method for random vibrations of hysteretic systems", *J. Eng. Mech. - ASCE,* **102**, 249-263.

Williams, D. and Godden, W.G. (1976), "Multidirectional seismic response of a curved highway bridge model", *Bull. NZ Soc. Earthq. Eng.*, **9**(2), 97-114.

Zhang, J., Deng, W. and Yue, Z. (2012), "Experimental Study about the Hysteretic Performance of the Pall-typed Piezoelectric Friction Damper", *TOCEJ*, **6**, 48-54.

CC